Gut-Microbial and -Metabolomic Signatures in the Prevention of Non-Alcoholic Fatty Liver Disease by *Lactobacillus Lactis* and *Pediococcus Pentosaceus*

Gi Soo Youn
Hallym University
Jeong Seok Yu
Seoul National University
Jieun Choi
Seoul National University
Yujin Kang
Seoul National University
Byung Yong Kim
ChunLab, Inc.
Tae-Sik Park
Gachon University
Byoung Kook Kim
Chong Kun Dang Bio Research Institute
Sang Jun Yoon
Hallym University
Na Young Lee
Hallym University
Ye Rin Choi
Hallym University
Hyeong Seob Kim
Hallym University
Haripriya Gupta
Hallym University
Hotaik Sung
Kyungpook National University
Sang Hak Han
Hallym University College of Medicine
Min Jea Shin
Hallym University
Dong Joon Kim

Hallym University

Ki Tae Suk (ktsuk@hallym.ac.kr)

Hallym University College of Medicine https://orcid.org/0000-0002-9206-9245

Do Yup Lee

Seoul National University

Research

Keywords: Non-alcoholic fatty liver disease, Microbiota, Gut-liver axis, Metabolites, Indole

Posted Date: September 10th, 2020

DOI: https://doi.org/10.21203/rs.3.rs-70769/v1

Abstract

Background: Despite a recent preventive evidence of *Lactobacillus* and *Pediococcus* on non-alcoholic fatty liver disease (NAFLD) progression, the underlying mechanistic is less understood. We explored the causality of *L. lactis* and *P. pentosaceus* on the gut-metabolomic modulation in the prevention of NAFLD progression in mouse model and subsequently discovered metabolic biomarkers based on NAFLD patients.

Results: Six-week-old male C57BL/6J mice were divided into 4 groups (control, Western diet [WD], and 2 WD with strains [*L. lactis* and *P. pentosaceus*]). Given completely reproduced data (liver/body ratio, pathology, and metagenomic profiles), comorbid etiologies including inflammation and diabetes were significantly amended by 2 strains. The comprehensive metabolomic profiles of the mouse cecum revealed unique compositional characteristic according to the groups. *L. lactis* and *P. pentosaceus* supplementation restored the dysregulation in short chain fatty acids (SCFAs), bile acids, and tryptophan metabolites. Indole derivatives (indole-3-acetic acid, indole-3-propionic acid, and indole-3-acrylic acid) showed anti-inflammatory activities by suppressing pro-inflammation cytokines. Human data (healthy control [n=30] and NAFLD patients [n=74]) were analyzed for clinical association and biomarker. The *Fermicutes*/*Bacteroidetes* ratio of NAFLD (4.3) was significantly higher compared with control (0.6) (p<0.05), accompanied by the dysregulation in the key metabolic signatures identified in mouse model. Metabolic panel with 5 stool metabolites (indole, bile acids, and SCFAs) revealed 0.868 (area under the curve; 95% CI 0.773-0.933) in the diagnosis of NAFLD.

Conclusion: *L. lactis* and *P. pentosaceus* ameliorate NAFLD by modulating gut metabolic environment, particularly the indole pathway, of the gut-liver axis. NAFLD progression was associated with metabolic deterioration in the SCFAs, bile acid, and indole pathways.

ClinicalTrials.gov: NCT04339725

Background

Non-alcoholic fatty liver disease (NAFLD) is one of the most common causes of chronic liver disease worldwide, and its incidence is constantly growing given its association with obesity, coronary artery disease, metabolic syndrome, and diabetes [1]. NAFLD encompasses fatty liver and non-alcoholic steatohepatitis (NASH). Currently, lifestyle change involving dietary regulation and exercise is the main therapeutic option for NAFLD [2]. Although many drugs have been developed for NAFLD, none of them have been approved by the US Food and Drug Administration due to difficulties in patient compliance and failure in clinical trials [3].

Recently studies have reported that the gut-microbiota is involved in liver disease along the gut-liver axis. The gut microbiota is closely related to the host, and changes in the gut microbiota are reported to play a crucial role in various human diseases [4]. There is a growing body of evidence that the gut microbiota exhibits a capacity to synthesize or produce metabolites [5]. Among gut microbiota-derived metabolites,

tryptophan metabolites have been shown to affect the development of NAFLD [6]. Indoles are major products of tryptophan-derived metabolites, and some indole family metabolites are reported to reduce the production of pro-inflammatory cytokines by downregulating macrophages, scavenging free radicals, and reducing oxidative stress [5, 7].

In our previous report, *Lactobacillus* and *Pediococcus* supplementation have been demonstrated to improve NAFLD by the modulating the gut microbiota and inflammation [8]. In addition, our preliminary study with strains licensed for human use and reproducibility experiments with selected strains have both shown promising results in Western diet (WD) induced NAFLD (Supplementary table 1 and supplementary Fig. 1). In this study, we comparably examined gut micro-environments of WD-induced NAFLD mice and of patients with NAFLD using metagenomics/metabolic profiling. We deepened the mechanistic understanding of the preventive effects of *L. lactis* and *P. pentosaceus* based on comprehensive examination on biochemical and pathology parameters.

Material And Methods

Strain preparation

Lactobacillus and *Bifidobacterium* used for the preliminary study were isolated from various source such as sour milk, cheese, healthy Korean adult feces and new-born's feces. *L. lactis* is lactic acid bacterium that was isolated from sour milk. *P. pentosaceus* (KCTC 18308P) is a strain of lactic acid bacterium that was isolated from finger millet (*Eleusine coracana*) gruel. *L.lactis* and *P. pentosaceus* were inoculated into a flask containing de Man, Rogosa, and Sharpe media (BD/Difco). The strains were incubated under anaerobic conditions at 37°C for 24 h. Stocks of each strain were prepared by mixing the culture broth with an equivalent 20% skim milk solution and then storing the mixture at -80°C.

Study design

Six-week-old specific pathogen free male C57BL/6J mice were purchased from Dooyeol Biotech (Seoul, Korea). Mice were divided into 4 groups (n=6-7/group): Normal control (NC), WD, WD with *L. lactis* (LL), and WD with *P. pentosaceus* (PP). The WD was purchased from Dooyeol Biotech WD (TD88137, Seoul, Korea) consisted of 42% fat, 42.7% carbohydrate, and 15% protein. *L. lactis* and *P. pentosaceus* were suspended in distilled water at a concentration of 10^9 CFU/g for 8 weeks (Fig. 1A).

Pathology

Specimens were fixed with 10% formalin and routinely embedded in paraffin, and the tissue sections were processed with hematoxylin and eosin, Masson's trichrome, and CD 68 staining. NAFLD activity score (NAS), an objective index for classifying the grade of fatty liver, was assessed [9]. All biopsy specimens were analyzed by a hepato-pathologist (S. H. H.).

Human data

A prospective cohort study was carried out between April 2017 and March 2020. A total of 104 patients comprising of healthy control (HC, n=30), NAFLD patients with normal liver enzymes (NAFLD-NLE, n=37), and NAFLD patients with elevated liver enzyme (NAFLD-ELE, n=37) were prospectively enrolled (ClinicalTrials.gov: NCT04339725). This study involved patients with liver disease who were followed-up at the hepatology department of Hallym University. The diseases of the patients were treated regardless of the study. This study was conducted in accordance with the ethical guidelines from the 1975 Helsinki Declaration, as reflected by a prior approval by the institutional review board for human research in hospitals participating in the trial (2016-134). Informed consent for enrollment was obtained from each participant. Patients with autoimmune hepatitis, malignancy, drug induced liver injury, and virus induced hepatitis were excluded.

Stool analysis for the metagenomics

Metagenomic DNA was extracted with a QIAamp stool kit (cat. no. 51504) and amplification of the V3 - V4 region of the bacterial 16S rRNA gene was conducted using barcoded universal primers. PCR was performed according to following steps: an initial denaturation at 95 °C for 5 min, 20 cycles of 95 °C for 30 seconds, 55 °C for 30 seconds, and 72 °C for 30 seconds, followed by a final extension at 72 °C for 10 min. Purification of the amplicons was conducted with an Agencourt AMPure XP system (Beckman, USA) and quantification of the purified amplicons was conducted using PicoGreen and quantitative PCR. After pooling of the barcoded amplicons, sequencing was carried out using a MiSeq sequencer on the Illumina platform (ChunLab Inc., Republic of Korea) according to the manufacturer's specification.

Microbiota profiling was conducted with the 16S-based Microbial Taxonomic Profiling platform of EzBioCloud Apps (ChunLab Inc., Republic of Korea). After taxonomic profiling of each sample, comparative analyzer of EzBioCloud Apps was used for the comparative analysis of the samples. Taxonomic assignment of the reads was conducted with ChunLab's 16S rRNA database (DB ver. PKSSU4.0) [10]. OTU picking was conducted with UCLUST and CDHIT with 97% of similarity cutoff [11]. Subsequently, Good's coverage, rarefaction, and alpha-diversity indices including ACE, Chao1, Jackknife, Shannon, Simpson, and NPShannon were calculated. Beta-diversity including PCoA and UPGMA clustering was shown in the comparative MTP analyzer. All 16S rRNA sequences were deposited in the ChunLab's EzBioCloud Microbiota database and sequencing reads of the 16S rRNA gene from this study were deposited in the NCBI Short Read Archive under the bioproject number PRJNA532302.

Metabolic profiling of mouse cecal samples and human stool samples

The metabolomic profiles of mouse cecum were acquired using a combination of GC-MS and two LC–MS methods. Cecal samples were thawed at 4 °C and mixed with 1.1 ml of cold extraction solvent (acetonitrile/water 1:1, v/v). The mixtures were vortexed for 1 minutes and sonicated for 5 minutes under ice and centrifuged at 13,200 rpm for 5 min at 4°C. Each supernatant (500 µl) was transferred into a new 2 ml tube for short chain fatty acids (SCFAs) analysis (Method 1, see the supplementary method for details)[12]. The rest of supernatant was mixed with 600 µl of cold extraction solvent (acetonitrile/methanol, 1:3, v/v). For the second extraction step, the mixtures were vortexed for 1 min and

centrifuged at 13,200 rpm for 5 minutes at 4 °C. The supernatants (500 μl) were aliquoted and transferred to new 1.5-ml tubes for gas-chromatography time-of-flight mass spectrometry (Method 2) and liquid-chromatography Orbitrap mass spectrometry (Method 3). The aliquots were concentrated to complete dryness using a speed vacuum concentrator (SCANVAC, Korea)[13]. Similarly, human stool metabolomic profiles were obtained based on Methods 1, 2 and 3. The cecal data acquired by GC-TOF MS has been retrieved from our previous study [8].

Real-time Reverse Transcription-Polymerase Chain Reaction (RT-PCR) Analysis

Isolation of total RNA from tissue was performed using a Trizol reagent kit (Invitrogen, Gaithersburg, MD, USA) according to the manufacturer's instructions. Aliquots of total RNA (2 μg) were converted to cDNA using cDNA reverse transcription kit (Applied Biosystems, Foster City, CA). The cDNA was amplified for quantitative PCR using the Luna® Universal Probe qPCR Master Mix (New England Biolabs Beverly, MA, USA) and each target specific probe-primer (Applied Biosystems, Foster City, CA).

ELISA

Tissue homogenates were incubated with PRO-PREP™ Protein Extraction Solution (iNtRON Biotechnology, Korea) at 4 °C for 30 min, vortexing 3 min after added stainless bead and then centrifuged at 10,000 g for 10 min. Resulting supernatants were harvested and analyzed for the levels of pro-inflammatory cytokines including TNF-α, IL-1β, and IL-6 were analyzed by enzyme-linked immunosorbent assay (R & D Systems, Minneapolis, MN), according to the manufacturer's instructions.

Western blots

Tissue homogenates were incubated with PRO-PREP™ Protein Extraction Solution (iNtRON Biotechnology, Korea) on ice for 30 min, vortex mixer 3 min after added stainless bead and then centrifuged at 10,000 g for 10 min. Thirty micrograms of proteins were resolved by 10% SDS-PAGE and transferred to nitrocellulose membranes. The blots were probed with the indicated primary antibodies RBP4 (1:1000, Abcam, Cambridge, MA, USA), phospho-NF-κB p65, MAPKs, phosphor-MAPKs, and GAPDH (1: 1000, Cell Signaling Technology, Beverly, MA, USA) followed by incubation with the corresponding horseradish peroxidase-conjugated secondary antibodies (1:10000 dillution). The membrane was reacted with the enhanced chemiluminescence (ECL) substrate solution and analyzed by Amersham Imager 680 (GE Healthcare UK Ltd, Buckinghamshire, UK).

Statistical analysis

One-way ANOVA, the Kruskal-Wallis test, and independent sample T-test were performed for the body weight, liver function test, histology analysis, RT-PCR, ELISA, and LAL test. A p value<0.05 was considered to indicate statistical significance. All statistical analyses were performed using GraphPad prism software ver. 8 (GraphPad Software Inc., San Diego, CA, USA). The statistical analyses were conducted on all continuous variables acquired from GC-MS and LC-MS. That analysis described to the supplemental information.

Results

L. lactis and *P. pentosaceus* suppress the progression of non-alcoholic fatty liver disease

The *L. lactis* (4.76±0.31) and *P. pentosaceus* (5.16±0.23) supplementations were associated with significant improvement in the liver/body weight ratio (%) when compared with that in the WD group (6.51±0.28)(Fig. 1B and 1C)(p<0.001). The 9-week WD induced steatosis and inflammation in the liver pathology whereas the two strain groups showed improvement in the pathologic findings. WD induced steatosis (2.67±0.52) was reduced in the strain groups (LL 1.33±0.52 and PP 1.83±0.41). Regarding the inflammation grade, the WD group (2.67±0.52) exhibited elevated scores in comparison to the strain groups which had a score of 1. The WD-induced increase of NAFLD activity score (NAS)(5.83±0.75) was significantly decreased in the LL (2.5±0.84) and PP (3.83±0.41) groups (Fig. 1D).

The mean levels of aspartate aminotransferase (AST) and alanine aminotransferase (ALT) in the LL (97±19 and 53±13 U/L) and PP (105±12 and 80±13 U/L) groups were lower than those in the WD group (198±29 U/L). The mean levels of bilirubin and cholesterol in the LL (0.71±0.15 and 155±27 mg/dl) and PP (0.62±0.10 and 219±17 mg/dl) groups were significantly lower than those in the WD group (1.17±0.35 and 313±24 mg/dl)(Fig. 1E). Pro-inflammatory cytokine levels were significantly decreased in the LL group in STAM model (Supplementary figure 2).

Western diet-induced dysbiosis is ameliorated by *L. lactis* and *P. pentosaceus* supplementation

In analysis of stool samples, the compositions of *Proteobacteria, Verrucomicrobia, Deferribacteres, Actinobacteria, Bacteroidetes, Firmicutes,* and ETC were different according to the diet groups (Fig. 2A). At the genus level, each group revealed different compositions (Fig. 2B). The *Firmicutes*-to-*Bacteroidetes* ratio (F/B ratio) has been broadly studied in human and mouse gut microbiotas [14]. The F/B ratio in the WD group (60.1) was decreased in the LL (17.8) and PP (13.6) groups (Fig. 2C). In the analytics for beta diversity for microbiota taxonomic profiling, each group showed a different location (Fig. 2D). WD-induced decrease in species richness and diversity index is not changed by strains supplementation (Fig. 2E). In a heatmap for the comparison of species, each groups was associated with different patterns compared with that of the WD group, and WD-induced changes in a heatmap for the functional biomarker expression is recovered by *L. lactis* and *P. pentosaceus* supplementation (Fig. 2F). *Lactobacillus* abundance was increased in the PP group. Also, significantly recovered *Bacteroides acidifaciens* abundance by LL group. That reported to may have potential for treatment of metabolic diseases such as diabetes and obesity[15](Supplementary figure 3A). The top 42 statistically significant markers not shown in Figure 2 are presented in supplementary table 2.

The composition of the gut-microbiota differs according to the progression of liver disease

In the analysis of human stool, the proportions of phyla were different according to the progression of liver diseases (Fig. 3A). In the taxonomic composition at the phylum level, *Firmicutes* abundance increased in the NAFLD-ELE group when compared with HC group. At the genus level, each group

revealed different compositions (Fig. 3B). *Bacteroidetes* abundances and the F/B ratio were significantly different between the HC, NAFLD-NLE, and NAFLD-ELE groups (Fig. 3C)(p<0.001). In the comparison for beta diversity, each group occupied a different area (Fig. 3D). The species richness and diversity indexes were significantly decreased according to disease progression (Fig. 3E). When looking at the heatmap for the comparison of species, each group demonstrated different patterns, and functional biomarkers were also expressed with different patterns (Fig. 3F). The top 38 statistically significant markers not shown in Figure 3 are presented in supplementary table 3. *Prevotella* was decreased as the disease progressed (Supplementary figure 3B).

Short chain fatty acids are characteristically altered by diet type and strain supplementation

Overall, the WD group was associated with significant decreases in the short chain fatty acids (SCFAs) except iso-valeric acid when compared with those in the NC, LL, and PP groups (p<0.05)(Fig. 4A). The LL group showed marginal differences after multiple comparison adjustment whereas the PP group presented significant differences in all SCFAs compared to the WD group. The differences were not significant between the two strains-supplemented groups (Supplementary table 4).

Subsequently, we analyzed SCFAs from NC (n=35) and NAFLD-ELE (n=26). Similarly, the levels of the main SCFAs were observed significantly lower levels in the patients with NAFLD-ELE than in the HCs (p<0.05)(Fig. 4B and supplementary table 4).

Comprehensive profiling of the mouse cecal metabolome shows unique different patterns among groups

To comprehensively profile cecal metabolic context, we performed untargeted and targeted metabolic profiling of cecal samples based on GC- and LC-MS analysis. The metabolomic profiles were analyzed for the NC, WD, LL, and PP groups. Metabolic features were assigned to 282 unique compounds based on reference comparisons, spectra library searching, and retention time indexes. The chemical ontology analysis classified the compounds, and approximately 50% of metabolites were categorized as organic acids and lipid molecules (Fig. 4C). The sub-categories of the major classes were as follows: carboxylic acids, fatty acyls, and steroids accounted for 60, 32, and 14 compounds, respectively (Supplementary table 5). Subsequent pathway analysis demonstrated a wide range of coverage, including amino acid metabolism, carbohydrate metabolism, and fatty acid metabolism (Supplementary figure 4A).

First, the metabolic phenotypes of the four groups were characterized by unsupervised multivariate statistics. Principal component analysis showed the distinctive clusters between the NC group and the others (Fig. 4D). We, then, evaluated cecal metabolomic traits that were altered by the WD as a baseline. A significant difference was found for a total of 135 compounds out of 282 (Supplementary table 6). 11 percent of metabolites were significantly enriched in the WD group, whereas 37 percent were depleted when compared to those in the NC group (Fig. 4E). The largest depletion was determined to be 5-hydroxyindole-3-acetic acid content in the WD group (Supplementary table 6). Other indole derivatives were concomitantly depleted including indole-3-propionic acid, methyl indole-3-acetic acid, indole-3-acetic acid, and indole-3-acrylic acid (Supplementary table 6). In addition, pathway overrepresentation analysis

implied repression of carbohydrate metabolism (Supplementary figure 4B). Taurine conjugated bile acids were the compound with highest increases in WD group compared to NC group. Taurocholic acid and taurochenodeoxycholic acid were associated 50-/43-fold increases in WD group compared to NC group, respectively. Other increases associated with WD group included enriched metabolites were glutamic acid, cholesterol, 2'-deoxycytidine, and glycocholic acid (>10-fold changes). Overall, the most significantly upregulated compounds were determined to be associated with amino acid metabolism and primary bile acid biosynthesis based on pathway analysis (Supplementary figure 4B, right panel).

Exploration of gut microbiota-derived remedial therapeutics: common metabolic signatures among the 3 groups relative to the Western diet group

We explored common metabolic features among the NC, LL, and PP groups in comparison to the WD group, which may determine which molecular phenomic signatures were microbiota-derived and potentially had roles in remediating NAFLD. The metabolic re-programming by the two strains were similar overall (Fig. 4E). To effectively identify the metabolic features, we constructed an integrated metabolic network that was tiered by chemical structural similarity and enzymatic reaction connectivity. To effectively identify the metabolic features, we constructed an integrated metabolic network (MetaMapp) that was tiered by chemical structural similarity (*Tanimoto* score) and enzymatic reaction connectivity (KEGG reaction pair). The network provided a general overview at the level of the metabolic module and comprehensive details at the individual metabolite level [13]. Overall, the LL and PP groups showed compatible patterns in major metabolic modules, which coincided with the similar levels of the preventive effect of WD-induced liver damage.

We further interrogated the common metabolites that were similarly regulated in the NC and strain-fed groups. A total of 33 metabolites showed similar patterns among the three groups when compared to those in the WD group (Fig. 5A and supplementary figure 5). The metabolic profiles of the 33 metabolites were associated with the highest discrimination among the three groups, the NC, strain-fed groups, and the WD group (Fig. 5B).

Compared to those in the WD group, gut-bacterial metabolites (indole-3-propionic acid and methyl indole-3-acetic acid) showed the highest fold-change in the NC and strain-fed groups (Fig. 5C and D). On contrary, indole-3-lactic acid and indole-3-pyruvic acid were exclusively different in the LL group and the PP group, respectively. Whereas indole-3-acrylic acid was highly abundant only in the NC group (Fig. 5E and supplementary table 7). Subsequently, we evaluated the indoles from human fecal samples and compared the levels between HC and patients with NAFLD-ELE. Indole-3-propionic acid was at significantly-reduced level in the patient group (Student's *t*-test, $p<0.01$). Indole-3-acrylic acid and indole-3-acetic acid were marginally reduced ($p=0.225,0.473$) whereas indole-3-lactic acid was moderately increased in the NAFLD patients compared to HC (Student's *t*-test, $p=0.100$) (Fig. 5F).

Bile acid homeostasis in the farnesoid X receptor pathway is altered by diet and is regulated by the tight junction of the intestine.

Primary BAs conjugated with taurine were most dramatically upregulated in the WD group, compared to those in the other groups (Fig. 6A). Glycocholic acid was significantly enriched in the WD group relative to that in the NC and LL groups. In contrast, secondary BAs following deconjugation/dehydroxylation of primary BAs presented a decreasing tendency in the WD group except taurodeoxycholic acid (supplementary table 6). Overall, the fecal BAs showed elevated levels in the patients diagnosed with NAFLD-ELE (Fig. 6B), which were not identical to the profiles of the cecal BAs in the WD group. Nonetheless, comparable dysregulation was identified for fecal taurocholic acid (p=0.05, FDR=0.1) and glycocholic acid (p=0.104, FDR=0.156) in the patients diagnosed with NAFLD-ELE (Fig. 6B). The deconjugated BAs (cholic acid and chenodeoxycholic acid) were the most significantly enriched in the patients, consistent with a previous report [16].

BA homeostasis is critically regulated by the farnesoid X receptor (FXR), which is activated by BAs [17]. The BA synthesis-, BA transport-, and hepatic acid regulation-related genes NCTP, Cyp7A1, SHP, and FXR were downregulated in the WD group. However, the LL and PP groups were associated with partial recovery of aforementioned downregulation (Fig. 6C).

We analyzed the expression of the tight junction occludin and ZO-1 genes. The LL and PP groups were shown with increased occludin and ZO-1 gene expression compared with that in the other groups (Fig. 6D). Caco-2 cells were cultured to complete confluence and co-incubated with a bacterial suspension in MEM for eight hours. The treatment of Caco-2 cells with LL and PP increased the trans-epithelial electrical resistance values by 2.3- and 1.9-fold, respectively, compared with those of non-treatment controls. And endotoxin analysis in serum was performed. The elevated levels of endotoxin in the WD group were reduced in the LL group. However, those in the PP group were not significant (Fig. 6E). These results suggest that LL and PP supplementation strengthened intestinal-barrier function and reduced bloodstream endotoxin infiltration from the intestine.

Carbohydrate metabolism was correspondingly altered according to the diet type. All monosaccharides were significantly more enriched in the NC group than in the WD group. Among the intestinal monosaccharides, glucose and xylose were significantly depleted in the WD group, respectively compared to those in the other groups (Fig. 6F). The strain-fed groups showed glucose levels equivalent to those in the NC group. Fructose was not differentially regulated among the WD groups, whereas galactose and mannose levels in the PP group were at comparable levels to those in the NC group (Supplementary table 8 and supplementary figure 6).

L. lactis and *P. pentosaceus* attenuate inflammation and insulin resistance in the liver

Altered metabolite composition due to gut microbiota dysbiosis can damage the liver and induce inflammation through the gut-liver axis. Elevated inflammatory cytokines, such as tumor necrosis factor (TNF)-α, interleukin (IL)-1β, and IL-6 in the WD group were significantly decreased via the LL and PP groups (Fig. 7A). Immunohistochemical analyses for CD68, a marker for macrophages, were performed in representative cases. The mean value of the positive-stained area measured in random areas of the liver was determined. The strain groups showed significant reduction in stained area compared to the area for

the WD group (Fig. 7B). Various MAPKs, such as p38, c-Jun NH2-terminal kinase and extracellular signal-regulated kinase participate in the expression of pro-inflammatory mediators during inflammatory responses [18]. Elevated activation of the MAPK-NF-kB pathway in the WD group was decreased in the LL and PP groups (Fig. 7C). Inflammation in adipose tissues is a mechanism to induce insulin resistance and is mediated by the activation of cellular stress-induced inflammatory signaling pathways. The pro-inflammatory adipokines retinol-binding protein 4 and leptin were elevated the WD group and significantly decreased the LL and PP groups. In addition, the anti-inflammatory adipokine adiponectin decreased in the WD group and was significantly elevated in the LL group compared with that in the WD group (Fig. 6D and E).

In vitro analysis of the anti-inflammatory response of tryptophan metabolites

We examined the involvement of indole compounds in regulation of pro-inflammatory cytokines such as TNF-α and IL-1β in LPS-stimulated macrophages. Raw264.7 cells were treated with LPS and indole-3-acetic acid (100 μM), indole-3-propionic acid (100 μM)[19], or indole-3-acrylic acid (500 μM)[20]. Indole compounds significantly decreased the expression of TNF-α, IL-1β, and IL-6 mRNA (Fig. 6F).

Biomarkers for non-alcoholic steatohepatitis

We performed binary logistic regression analysis to examine whether a single molecule or composed set of metabolites can predict NAFLD-ELE (n=45) over HCs (n=35). Based on the metabolites (SCFAs, indoles, and BAs), we applied receiver operating characteristic (ROC) curve analysis for accuracy, specificity, and sensitivity. The area under the curve (AUC) for indole-3-propionic acid was 0.782 (95% CI, 0.676-0.867) (Fig. 8A). A linear composite of three metabolites (indole-3-propionic acid, chenodeoxycholic acid, and butyric acid) showed good discrimination power (AUC [95% CI]: 0.846 [0.748-0.917]. A metabolic panel with six metabolites reached an AUC of 0.868.

Discussion

Our current investigation is the first report on the accomplishment of the comprehensive stool metabolomics-based elucidation of the preventive mechanism of strain-supplementation therapy for NAFLD. Besides, we link the metagenomic and metabolomic features of the mouse model to human data, which leads to the discovery of potential biomarker, precisely diagnosing NAFLD progression.

Supplementation with *L. lactis* and *P. pentosaceus* strains are known to be associated with beneficial effects in various diseases such as enteritis, inflammation, and hypertension [21, 22]. *Pediococcus* inactivated hepatic stellate cells among with a decreasing hepatic inflammatory response by via suppression of macrophages and inflammatory cytokines [23]. In this study, *L. lactis* and *P. pentosaceus* were found to attenuate inflammation and insulin resistance in the liver. Overall, *L. lactis* and *P. pentosaceus* supplementation should be considered a potentially effective therapeutic options in the treatment of NAFLD.

WD induces dysbiosis and elevation of endotoxin levels in the gut [8]. These bacterial endotoxins activate macrophages by engaging Toll-like receptor 4. Macrophages produce inflammatory cytokines or chemokines which lead to liver damage through the MAPK-NF-kB signaling pathway. Our study also demonstrated that the WD is related with endotoxemia, alteration of microbiota composition, macrophage related elevation of cytokine levels, and MAPK-NF-kB signaling. In addition, *P. pentosaceus* decreased serum endotoxin level via restoring gut-permeability and curved release of pro-inflammatory cytokines by inactivating MAPK-NF-kB signaling.

In our study, *L. lactis* and *P. pentosaceus* supplementation significantly decreased the L/B ratio, NAS score, and serum chemistry markers as compared to the WD group. Previous studies suggested that the gut-liver axis plays an important role in the pathophysiology of NAFLD and that probiotics can modulate the elements of the gut-liver axis, especially the gut microbiota [8, 24]. Altogether, our results showed that *L. lactis* and *P. pentosaceus* supplementation might be effective for bringing about weight reduction and histologic improvement in patients with NAFLD.

Regarding metagenomics, it is well-known that WD influences the composition of the intestinal microflora in animals, and this difference is also found in patients with NAFLD [8]. In our research, administration of different strains resulted in differential composition of the microbiota. Whether the alteration of intestinal microbiota is a result of disease progression or compensatory reaction to disease is not clearly understood; more research is needed to understand the mechanism or ecosystem of these strains. The metagenomic profiles did not reveal a correspondence in the proportions of the gut microbiota between the normal control and probiotic-fed groups. This inequivalence implies that the common molecular mechanism drives the protective effects of probiotic supplementation on WD-induced NAFLD.

Indeed, a growing evidence implicates gut microbiota-derived metabolites as active modulators, encompassing diet, microorganisms, and the host, attributed to causal functionality, including SCFAs and tryptophan metabolites [19, 25]. Tryptophan metabolites in particular have been shown to affect the development of NAFLD by altering the composition of the gut microbiota [5, 26]. Indole compounds are major products of tryptophan-derived metabolites, and include indole-3-acrylic acid, indole-3-acetic acid, and indole-3-propionic acid [5, 7, 20]. In a previous study, indole-3-acrylic acid was reported to promote intestinal epithelial barrier function and mitigate inflammatory responses via NRF2 activation [19]. Indole-3-acetate is associated with attenuation of indicators of inflammation in macrophages and cytokine-mediated lipogenesis in hepatocytes [20]. Additionally, indole-3-propionic acid has been found to improve HFD-induced intestinal epithelial barrier damage and inhibits endotoxin-induced production of pro-inflammatory cytokines via inactivation of NF-κB signaling [27]. Indeed, our metabolomic analysis revealed that the indole compounds were differentially regulated by the *L. lactis* and *P. pentosaceus* and the levels of indole compounds in the probiotic-feeding groups were the comparable levels to those of normal control. Particularly, indole-3-propionic acid was associated with the highest fold-change when normal control and two probiotic-feeding groups were compared with the western diet group. The differential regulation coincided with results for the NAFLD-ELE patients. Accordingly, we examined the functionality of three indole compounds, which were linked to suppression of cytokines such as TNF-α

and IL-1β, in LPS-treated macrophages. These results imply that a diet with *L. lactis* and *P. pentosaceus* at least partially protects against NAFLD progression via the production of anti-inflammatory metabolites such as indole compounds.

BAs have direct or indirect antimicrobial effects and modulate the composition of the microbiota, which in turn has a role in regulating the size and composition of the BA pool [28]. BA homeostasis is critically regulated by FXR, which is activated by BAs. FXR is known to exert tissue-specific effects in regulating BA synthesis and transport [17]. Previous studies showed that mice with FXR deficiency were afflicted with hepatic steatosis as well as glucose and insulin intolerance, the main hallmarks of NAFLD in humans [29, 30]. There have been incoherent results regarding BAs, implicating the complexity in which different spatial and temporal examinations have been performed under non-identical experimental settings. For instance, there have been a relatively few number of investigations on intestinal BAs. Nonetheless, the WD-induced NAFLD in our study was best characterized by dysregulation of unconjugated BAs, which is consistent with other recent studies [31]. Besides, our results clearly revealed that the WD-induced dysregulation of BAs was largely restored by the strains administration. The fecal BAs in the patients with NAFLD-ELE did not share identical pattern compared to that of WD-induced NAFLD mouse model; however, the general trend was similar in regards to alteration of unconjugated BAs by WD. In particular, the diet-induced accumulation of taurocholic acid has been reported to perturb gut microbial symbiosis in a mouse model [32, 33] and to stimulate hepatic inflammation and fibrosis [34].

It is plausible that a WD induces severe reduction of microbial diversity, which leads to the depleted SCFAs content [35] triggering accelerated glucose consumption by host enterocytes and colonocytes to compensate for depletion of the main energy sources. Accordingly, we observed a decreased glucose level in the WD group, which was ameliorated by strains supplementation, resulting in glucose levels equivalent to those in the normal control group. It is also worth noting that a significantly higher content of mannose was identified in the normal control and strain-fed groups. The beneficial effect of dietary supplementation of mannose is associated with the modulation of gut microbiome, leading to prevention of diet-induced obesity and amended host metabolism [36].

In our study, the diagnostic model utilizing biomarkers were shown to have promising results in AUC (0.782–0.868). Although there are few studies related to biomarkers through fecal metabolomics analysis of nonalcoholic fatty liver disease with elevated liver enzymes, a recent study using microbiota data demonstrated diagnostic accuracy (AUC 0.87) for detecting fibrosis in NASH [37]. If the method using feces overcomes cost and time challenges, it will be used in various fields of liver disease in the future.

Conclusion

In summary, we investigated the intestinal microbial normalization and anti-inflammatory effects of *L. lactis* and *P. pentosaceus* in the NAFLD mouse model. Diet with the *L. lactis* and *P. pentosaceus* inhibited NAFLD progression via normalization of BA composition, which in turn was achieved by modulation of

gut microbiota composition and production of anti-inflammatory metabolites such as indole compounds (Fig. 8B).

Abbreviations

Non-alcoholic fatty liver disease, NAFLD; Non-alcoholic steatohepatitis, NASH; Short chain fatty acids, SCFAs; NAS, NAFLD activity score; normal diet group, NC; Western diet group, WD; Western diet group treated with *L. lactis*, LL; Western diet group treated with *P. pentosaceus*, PP; Healthy control, HC; NAFLD elevated liver enzymes, NAFLD-ELE; NAFLD non-elevated liver enzymes, NAFLD-NLE; Farnesoid X receptor, FXR; Toll-like receptor 4, TLR4; Aspartate aminotransferase, AST; Alanine aminotransferase, ALT; Tumor necrosis factor, TNF; Interleukin, IL; Liver weight / Body weight ratio, L/B ratio

Declarations

Ethics approval and consent to participate

The animals received humane care and all procedures were performed in accordance with National Institutes of Health Guidelines for the Care and Use of Laboratory Animals. All procedures were approved by the Institutional Animal Care and Use Committee of the College of Medicine, Hallym University (2018-04).

Consent for publication

Not applicable.

Availability of data and material

The datasets (16S rRNA gene-based microbiome taxonomic profiling) supporting the conclusions of this article are available in the EzBioCloud (https://www.ezbiocloud.net) under ChunLab, Inc. All 16S rRNA sequences were deposited in the ChunLab's EzBioCloud Microbiota database and sequencing reads of the 16S rRNA gene from this study were deposited in the NCBI Short Read Archive under the bioproject number PRJNA532302.

Competing interests

The authors declare that they have no competing interests.

Financial support

This research was supported by Hallym University Research Fund, the Basic Science Research Program through the National Research Foundation of Korea (NRF) funded by the Ministry of Education, Science and Technology (NRF-2018M3A9F3020956, NRF-2019R1I1A3A01060447, and NRF-2020R1A6A1A03043026) and Hallym University Research Fund 2018 (HURF-2018-67).

Conflicts of interest

Authors B.Y.K. was employed by company ChunLab, Inc. Authors B.K.K. was employed by company Chong Kun Dang Bio. All other authors attest that there are no commercial associations that might be a conflict of interest in relation to the submitted manuscript.

Author's contribution

K.T.S., D.Y.L., B.Y.K., T.S.P., and B.K.K. conceived and designed the study; G.S.Y. and J.S.Y. performed, analyzed and interpreted most of the experiments; H.S. provided technical assistance; analysis and interpretation of data, collection and assembly of data, and drafting the article. K.T.S. and D.Y.L. critically revised the manuscript and approved final article. Other authors: Provision of study materials or results

References

1. Suk KT, Kim DJ: Gut microbiota: novel therapeutic target for nonalcoholic fatty liver disease. Expert Rev Gastroenterol Hepatol 2019, 13:193-204.
2. Hossain N, Kanwar P, Mohanty SR: A Comprehensive Updated Review of Pharmaceutical and Nonpharmaceutical Treatment for NAFLD. Gastroenterol Res Pract 2016, 2016:7109270.
3. Sanyal AJ, Chalasani N, Kowdley KV, McCullough A, Diehl AM, Bass NM, Neuschwander-Tetri BA, Lavine JE, Tonascia J, Unalp A, et al: Pioglitazone, vitamin E, or placebo for nonalcoholic steatohepatitis. N Engl J Med 2010, 362:1675-1685.
4. Lindheim L, Bashir M, Munzker J, Trummer C, Zachhuber V, Leber B, Horvath A, Pieber TR, Gorkiewicz G, Stadlbauer V, Obermayer-Pietsch B: Alterations in Gut Microbiome Composition and Barrier Function Are Associated with Reproductive and Metabolic Defects in Women with Polycystic Ovary Syndrome (PCOS): A Pilot Study. PLoS One 2017, 12:e0168390.
5. Zhou D, Fan JG: Microbial metabolites in non-alcoholic fatty liver disease. World J Gastroenterol 2019, 25:2019-2028.
6. Canfora EE, Meex RCR, Venema K, Blaak EE: Gut microbial metabolites in obesity, NAFLD and T2DM. Nat Rev Endocrinol 2019, 15:261-273.
7. Konopelski P, Konop M, Gawrys-Kopczynska M, Podsadni P, Szczepanska A, Ufnal M: Indole-3-Propionic Acid, a Tryptophan-Derived Bacterial Metabolite, Reduces Weight Gain in Rats. Nutrients 2019, 11.
8. Lee NY, Yoon SJ, Han DH, Gupta H, Youn GS, Shin MJ, Ham YL, Kwak MJ, Kim BY, Yu JS, et al: Lactobacillus and Pediococcus ameliorate progression of non-alcoholic fatty liver disease through modulation of the gut microbiome. Gut Microbes 2020:1-18.
9. Kleiner DE, Brunt EM, Van Natta M, Behling C, Contos MJ, Cummings OW, Ferrell LD, Liu YC, Torbenson MS, Unalp-Arida A, et al: Design and validation of a histological scoring system for nonalcoholic fatty liver disease. Hepatology 2005, 41:1313-1321.

10. Yoon SH, Ha SM, Kwon S, Lim J, Kim Y, Seo H, Chun J: Introducing EzBioCloud: a taxonomically united database of 16S rRNA gene sequences and whole-genome assemblies. Int J Syst Evol Microbiol 2017, 67:1613-1617.
11. Edgar RC: Search and clustering orders of magnitude faster than BLAST. Bioinformatics 2010, 26:2460-2461.
12. Han J, Lin K, Sequeira C, Borchers CH: An isotope-labeled chemical derivatization method for the quantitation of short-chain fatty acids in human feces by liquid chromatography-tandem mass spectrometry. Anal Chim Acta 2015, 854:86-94.
13. Park SJ, Lee J, Lee S, Lim S, Noh J, Cho SY, Ha J, Kim H, Kim C, Park S, et al: Exposure of ultrafine particulate matter causes glutathione redox imbalance in the hippocampus: A neurometabolic susceptibility to Alzheimer's pathology. Sci Total Environ 2020, 718:137267.
14. Koliada A, Syzenko G, Moseiko V, Budovska L, Puchkov K, Perederiy V, Gavalko Y, Dorofeyev A, Romanenko M, Tkach S, et al: Association between body mass index and Firmicutes/Bacteroidetes ratio in an adult Ukrainian population. BMC Microbiol 2017, 17:120.
15. Yang JY, Lee YS, Kim Y, Lee SH, Ryu S, Fukuda S, Hase K, Yang CS, Lim HS, Kim MS, et al: Gut commensal Bacteroides acidifaciens prevents obesity and improves insulin sensitivity in mice. Mucosal Immunol 2017, 10:104-116.
16. Jahn D, Geier A: Bile acids in nonalcoholic steatohepatitis: Pathophysiological driving force or innocent bystanders? Hepatology 2018, 67:464-466.
17. Zhu Y, Liu H, Zhang M, Guo GL: Fatty liver diseases, bile acids, and FXR. Acta Pharm Sin B 2016, 6:409-412.
18. Kaminska B: MAPK signalling pathways as molecular targets for anti-inflammatory therapy–from molecular mechanisms to therapeutic benefits. Biochim Biophys Acta 2005, 1754:253-262.
19. Wlodarska M, Luo C, Kolde R, d'Hennezel E, Annand JW, Heim CE, Krastel P, Schmitt EK, Omar AS, Creasey EA, et al: Indoleacrylic Acid Produced by Commensal Peptostreptococcus Species Suppresses Inflammation. Cell Host Microbe 2017, 22:25-37 e26.
20. Krishnan S, Ding Y, Saedi N, Choi M, Sridharan GV, Sherr DH, Yarmush ML, Alaniz RC, Jayaraman A, Lee K: Gut Microbiota-Derived Tryptophan Metabolites Modulate Inflammatory Response in Hepatocytes and Macrophages. Cell Rep 2018, 23:1099-1111.
21. Ghouri YA, Richards DM, Rahimi EF, Krill JT, Jelinek KA, DuPont AW: Systematic review of randomized controlled trials of probiotics, prebiotics, and synbiotics in inflammatory bowel disease. Clin Exp Gastroenterol 2014, 7:473-487.
22. Jauhiainen T, Ronnback M, Vapaatalo H, Wuolle K, Kautiainen H, Groop PH, Korpela R: Long-term intervention with Lactobacillus helveticus fermented milk reduces augmentation index in hypertensive subjects. Eur J Clin Nutr 2010, 64:424-431.
23. Shi D, Lv L, Fang D, Wu W, Hu C, Xu L, Chen Y, Guo J, Hu X, Li A, et al: Administration of Lactobacillus salivarius LI01 or Pediococcus pentosaceus LI05 prevents CCl4-induced liver cirrhosis by protecting the intestinal barrier in rats. Sci Rep 2017, 7:6927.

24. Gupta H, Youn GS, Shin MJ, Suk KT: Role of Gut Microbiota in Hepatocarcinogenesis. Microorganisms 2019, 7.
25. Koh A, De Vadder F, Kovatcheva-Datchary P, Backhed F: From Dietary Fiber to Host Physiology: Short-Chain Fatty Acids as Key Bacterial Metabolites. Cell 2016, 165:1332-1345.
26. Liang H, Dai Z, Liu N, Ji Y, Chen J, Zhang Y, Yang Y, Li J, Wu Z, Wu G: Dietary L-Tryptophan Modulates the Structural and Functional Composition of the Intestinal Microbiome in Weaned Piglets. Front Microbiol 2018, 9:1736.
27. Zhao ZH, Xin FZ, Xue Y, Hu Z, Han Y, Ma F, Zhou D, Liu XL, Cui A, Liu Z, et al: Indole-3-propionic acid inhibits gut dysbiosis and endotoxin leakage to attenuate steatohepatitis in rats. Exp Mol Med 2019, 51:1-14.
28. Jia W, Xie G, Jia W: Bile acid-microbiota crosstalk in gastrointestinal inflammation and carcinogenesis. Nat Rev Gastroenterol Hepatol 2018, 15:111-128.
29. Ma Y, Huang Y, Yan L, Gao M, Liu D: Synthetic FXR agonist GW4064 prevents diet-induced hepatic steatosis and insulin resistance. Pharm Res 2013, 30:1447-1457.
30. Yao J, Zhou CS, Ma X, Fu BQ, Tao LS, Chen M, Xu YP: FXR agonist GW4064 alleviates endotoxin-induced hepatic inflammation by repressing macrophage activation. World J Gastroenterol 2014, 20:14430-14441.
31. Gupta B, Liu Y, Chopyk DM, Rai RP, Desai C, Kumar P, Farris AB, Nusrat A, Parkos CA, Anania FA, Raeman R: Western diet-induced increase in colonic bile acids compromises epithelial barrier in nonalcoholic steatohepatitis. FASEB J 2020, 34:7089-7102.
32. Devkota S, Wang Y, Musch MW, Leone V, Fehlner-Peach H, Nadimpalli A, Antonopoulos DA, Jabri B, Chang EB: Dietary-fat-induced taurocholic acid promotes pathobiont expansion and colitis in Il10-/- mice. Nature 2012, 487:104-108.
33. Ridlon JM, Wolf PG, Gaskins HR: Taurocholic acid metabolism by gut microbes and colon cancer. Gut Microbes 2016, 7:201-215.
34. Janssen AWF, Houben T, Katiraei S, Dijk W, Boutens L, van der Bolt N, Wang Z, Brown JM, Hazen SL, Mandard S, et al: Modulation of the gut microbiota impacts nonalcoholic fatty liver disease: a potential role for bile acids. J Lipid Res 2017, 58:1399-1416.
35. Nagpal R, Wang S, Ahmadi S, Hayes J, Gagliano J, Subashchandrabose S, Kitzman DW, Becton T, Read R, Yadav H: Human-origin probiotic cocktail increases short-chain fatty acid production via modulation of mice and human gut microbiome. Sci Rep 2018, 8:12649.
36. Sharma V, Smolin J, Nayak J, Ayala JE, Scott DA, Peterson SN, Freeze HH: Mannose Alters Gut Microbiome, Prevents Diet-Induced Obesity, and Improves Host Metabolism. Cell Rep 2018, 24:3087-3098.
37. Schwimmer JB, Johnson JS, Angeles JE, Behling C, Belt PH, Borecki I, Bross C, Durelle J, Goyal NP, Hamilton G, et al: Microbiome Signatures Associated With Steatohepatitis and Moderate to Severe Fibrosis in Children With Nonalcoholic Fatty Liver Disease. Gastroenterology 2019, 157:1109-1122.

Figures

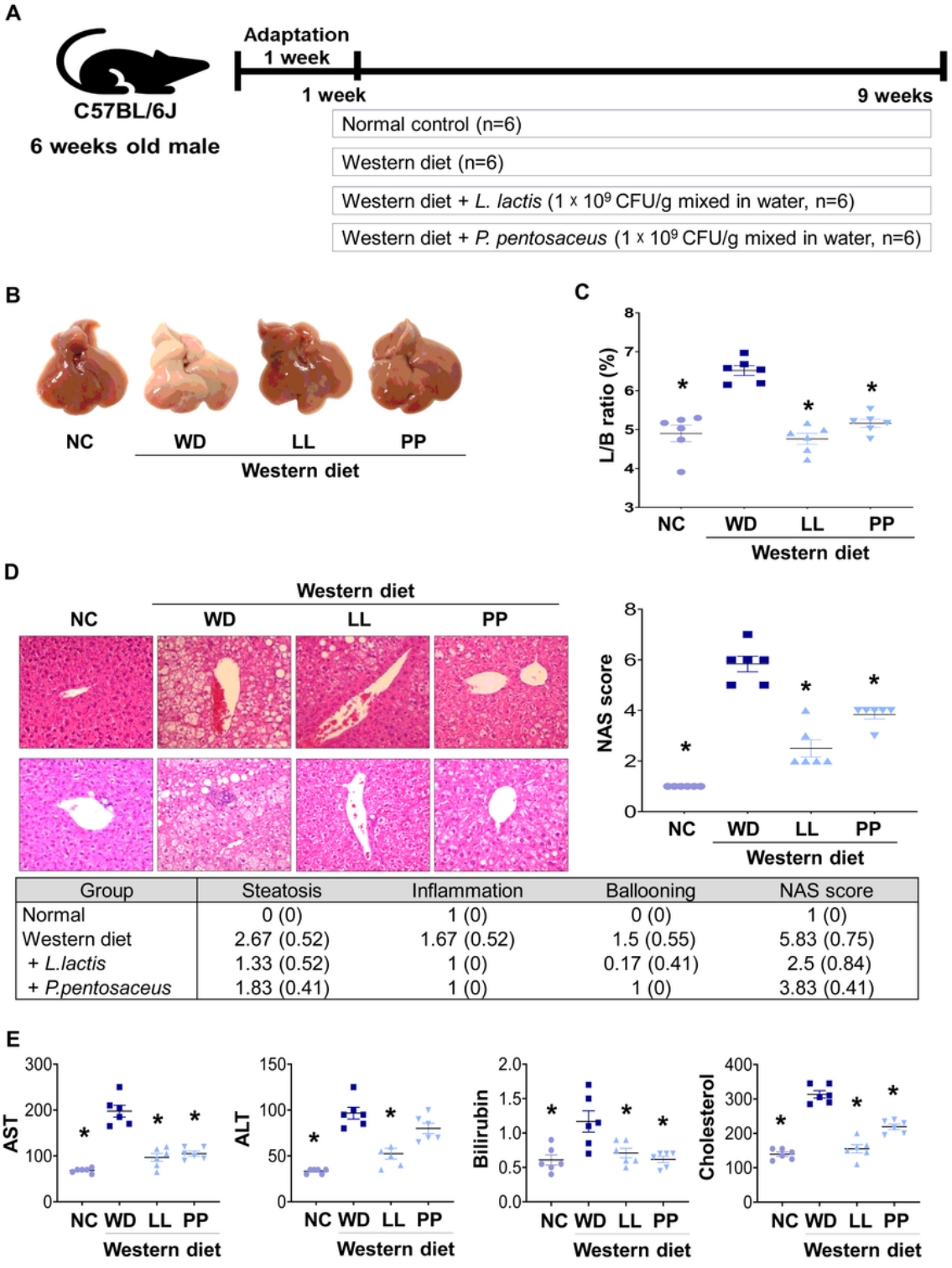

Group	Steatosis	Inflammation	Ballooning	NAS score
Normal	0 (0)	1 (0)	0 (0)	1 (0)
Western diet	2.67 (0.52)	1.67 (0.52)	1.5 (0.55)	5.83 (0.75)
+ *L.lactis*	1.33 (0.52)	1 (0)	0.17 (0.41)	2.5 (0.84)
+ *P.pentosaceus*	1.83 (0.41)	1 (0)	1 (0)	3.83 (0.41)

Figure 1

Effect of Lactobacillus and Pediococcus on the Western diet-induced liver disease. (A) Experiment design of WD model. (B) Gross specimen of mice liver. (C) L/B ratio. (D) Pathological effects of probiotics on the

liver. Hematoxylin and eosin staining of liver sections were analyzed (x 20) and analyze to NAS. (E) Liver function test and cholesterol level of mice. *p<0.05 as compared with WD.

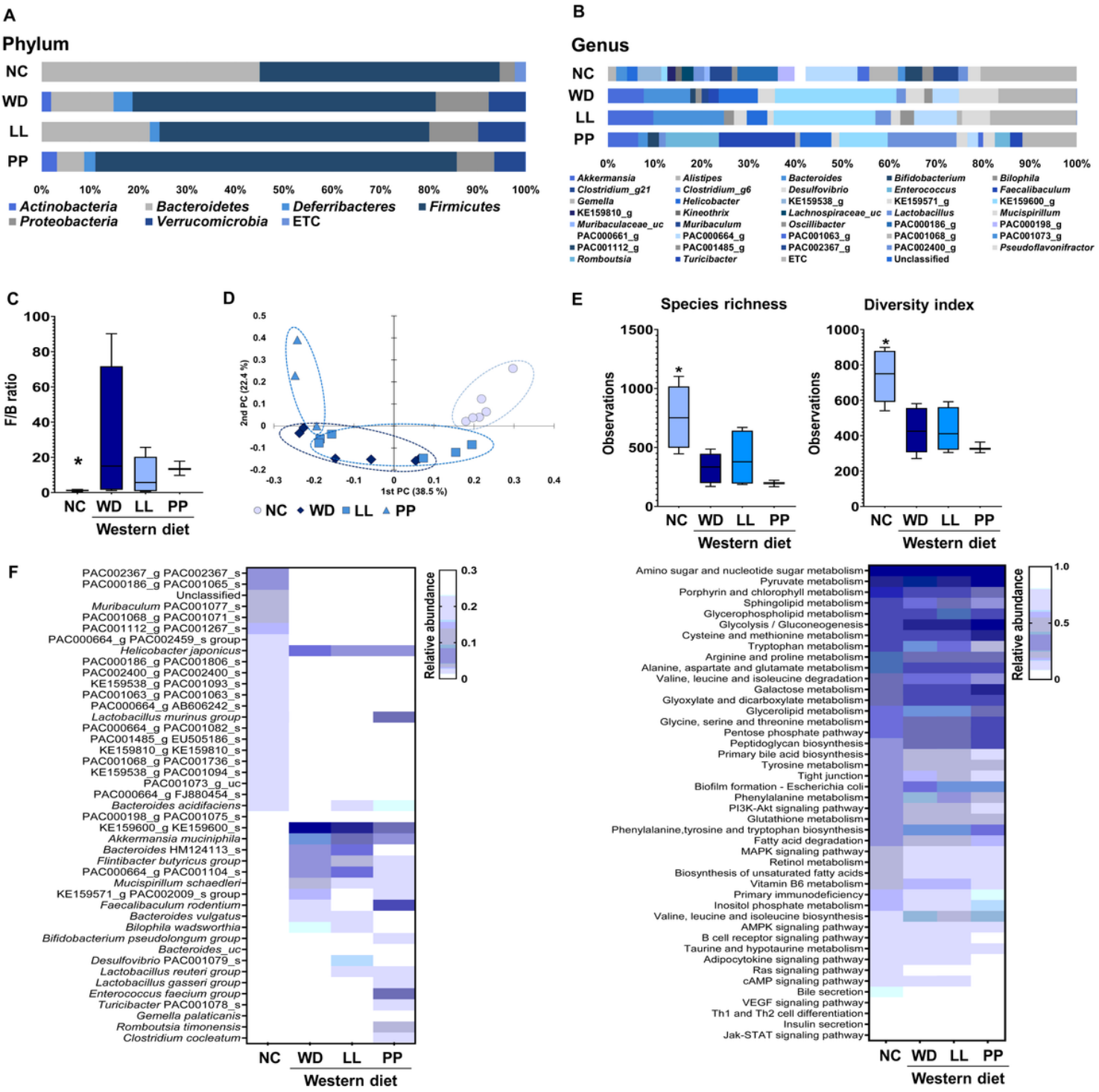

Figure 2

Microbiota composition analysis and related signaling pathways analysis in fecal samples in mouse fecal samples. (A) Phylum analysis. (B) Genus analysis. (C) Relative F/B ratio. (D) Beta-diversity analysis by UniFrac. (E) Alpha diversity analysis. (F) Heatmap for species analysis, and functional biomarker analysis. *p<0.05 as compared with WD.

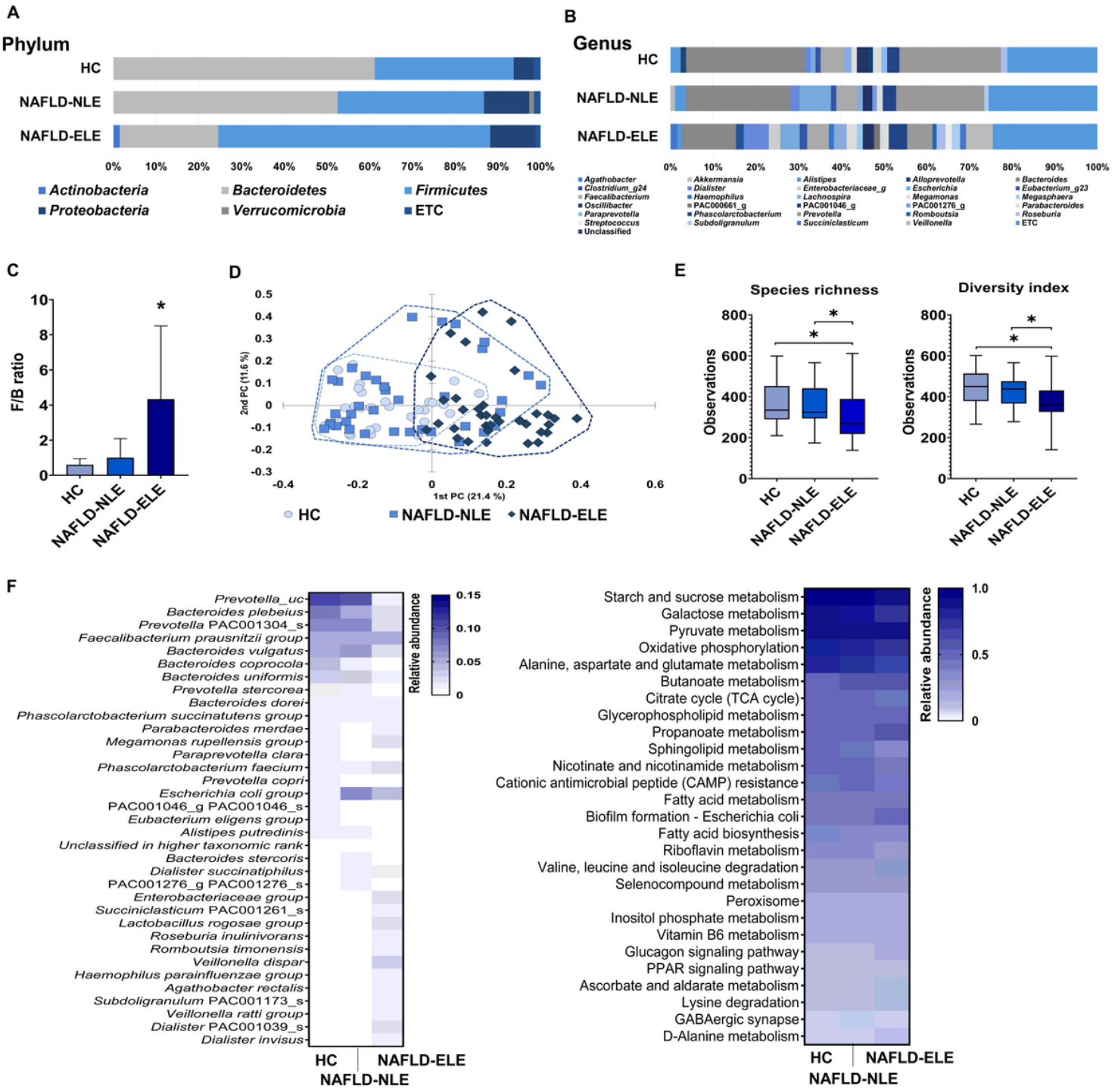

Figure 3

Microbiota composition analysis and related signaling pathways analysis in fecal samples in human fecal samples. (A) Phylum analysis. (B) Genus analysis. (C) Relative F/B ratio. (D) Beta-diversity analysis by UniFrac. (E) Alpha diversity analysis. (F) Heatmap for species analysis, and functional biomarker analysis. *p<0.05 as compared with HC.

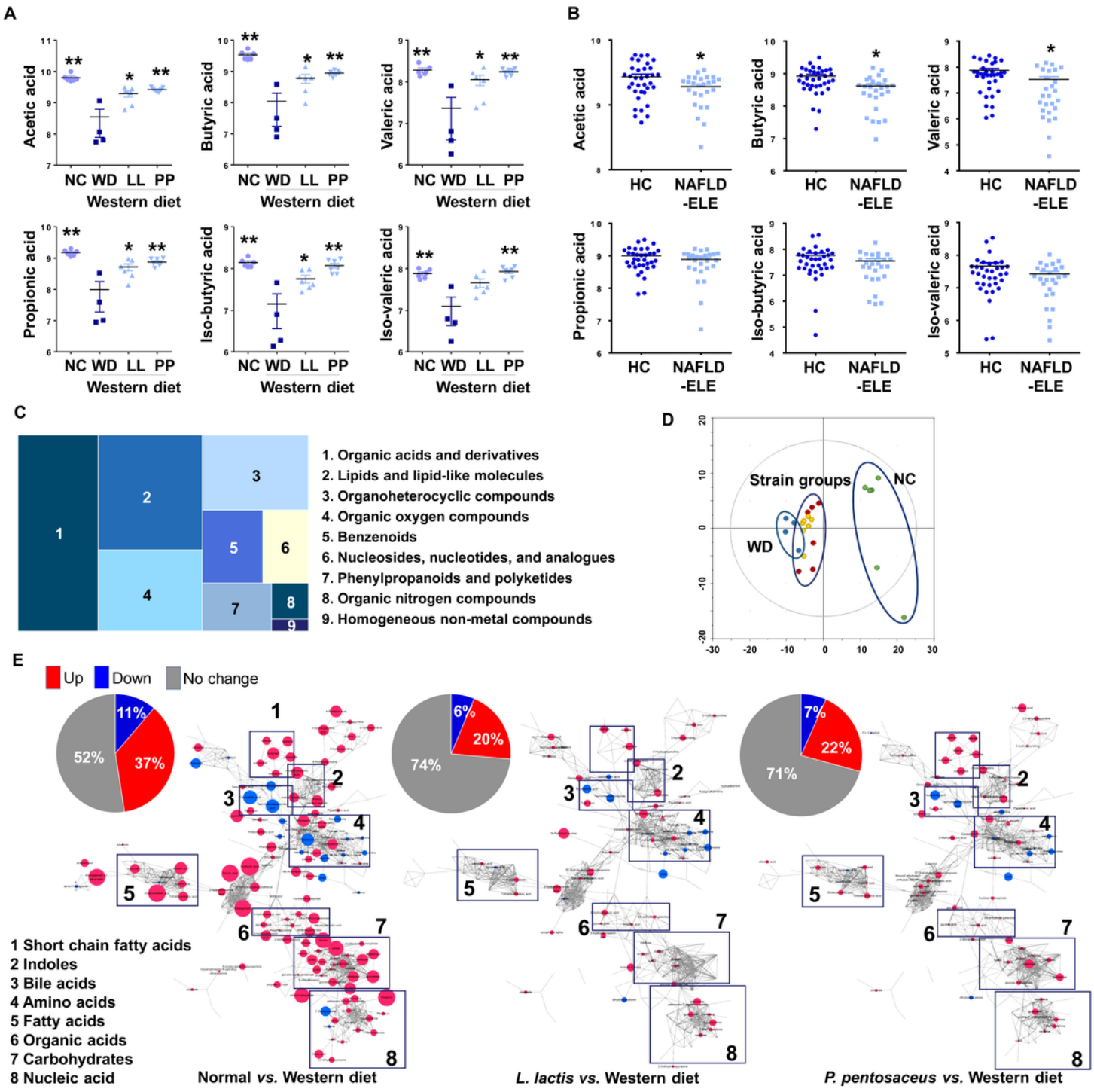

Figure 4

Cecal metabolomic alteration according to different diet types and probiotic supplementation. (A) The levels of cecal SCFAs in different diet groups (n=4-7). *p<0.05 as compared with WD. **p<0.05 as compared with WD group by nonparametric analysis. (B) The levels of human fecal SCFAs in 2 different groups, HC (n=35) and the patients with NAFLD-ELE (n=26). *p<0.05 as compared with HC. **p<0.05 as compared with HC after multiple comparison adjustment by false discovery rate. (C) Chemical classification of identified metabolites in mouse cecum (http://www.hmdb.ca). A total of 256 compounds

(91%) are categorized into 9 super classes. (D) The score scatter plot of 282 cecal metabolites by principal component analysis. Most variation was imposed by diet types (t1=30.8%). (E) Overview of the metabolic features. Pie charts present the number of metabolites that were significantly different in other groups, respectively compared to WD (p<0.05). Red and blue colors present significantly higher or lower abundant in other groups, respectively compared to WD (p<0.05).

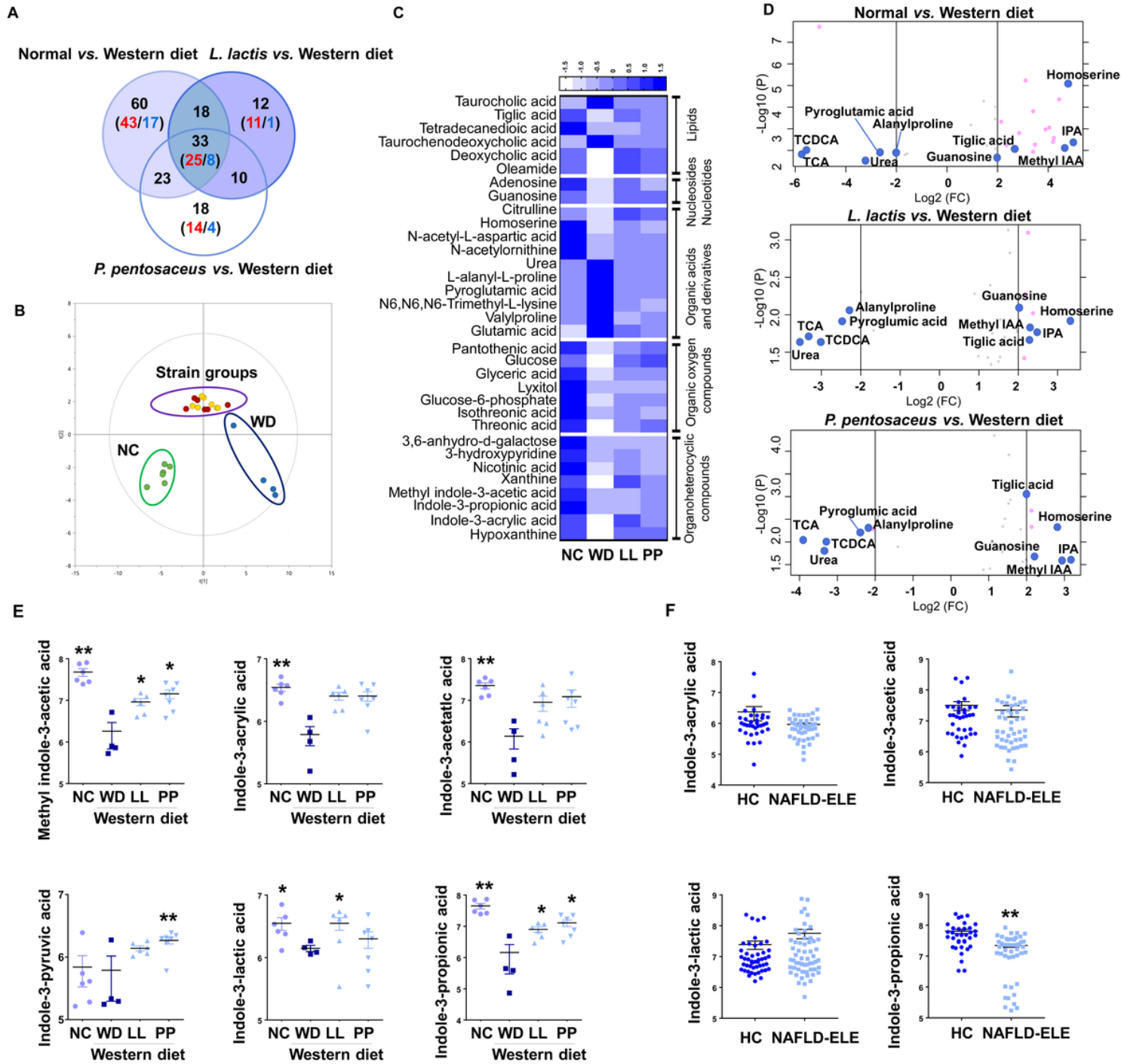

Figure 5

Common metabolic signatures that potentiate the preventive effects by probiotic-supplementation. (A) The metabolites that show common abundance pattern in other groups compared to WD group. A total of 33 metabolites are significantly different in all three groups. (B) The score scatter plot of the 33 cecal metabolites by principal component analysis. (C) Heatmap of auto-scaled abundances of the common metabolites. (D) Volcano plot of the common metabolites (33 metabolites). (E) The levels of cecal indole and indole derivatives in different diet groups (n=4-7). *p<0.05 as compared with WD group by Mann-Whitney U test. **p<0.05 as compared with WD group by nonparametric analysis (p<0.05). (F) The levels of human fecal indoles in 2 different groups, normal control (n=35) and the patients with NAFLD-ELE (n=45). *p<0.05 as compared with HC. **p<0.05 as compared with HC after multiple comparison adjustment by false discovery rate.

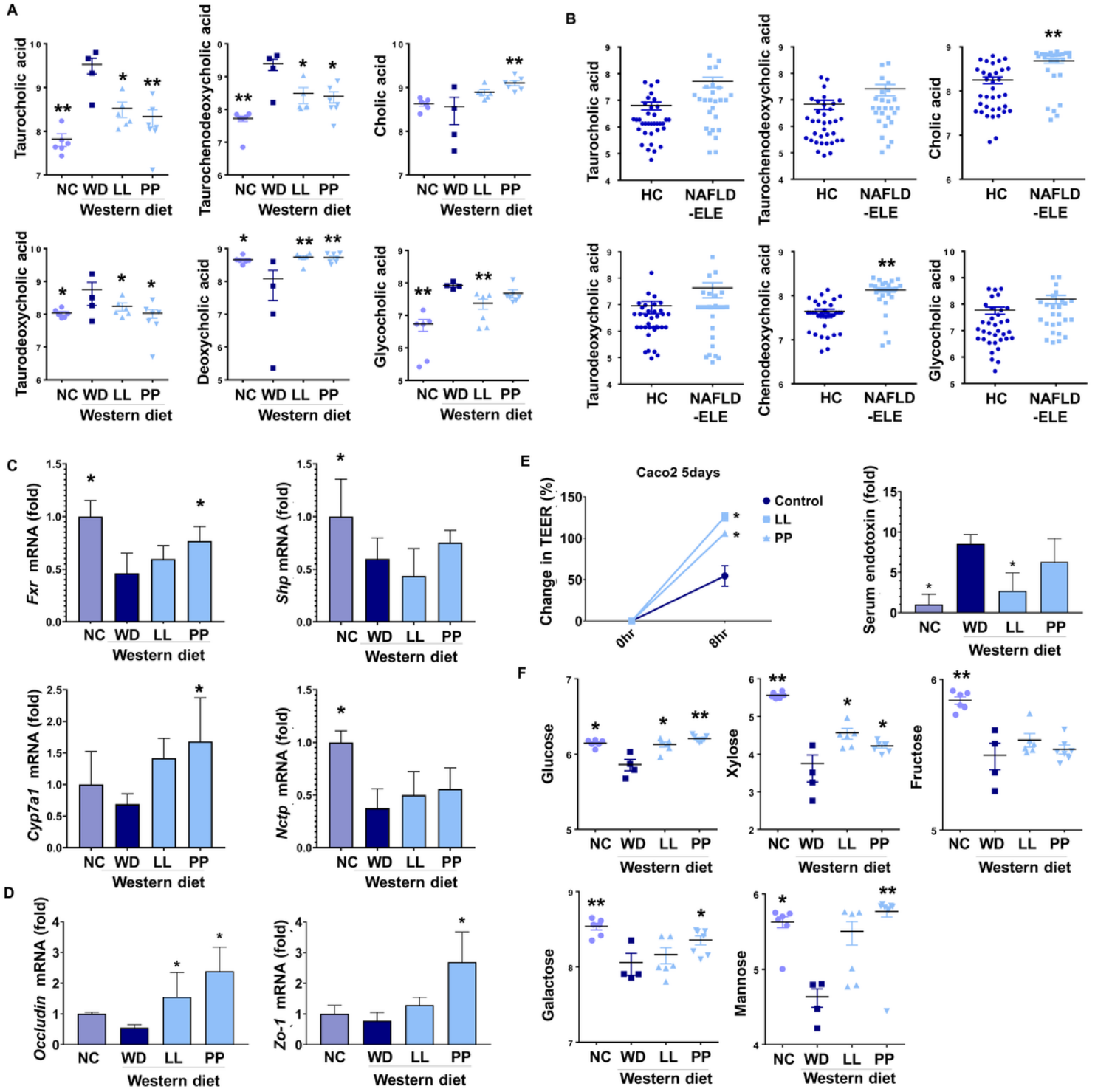

Figure 6

Bile acid composition change and intestine barrier protection effects by probiotic-supplementation. (A) The levels of BAs in different diet groups (n=4-7). (B) The levels of fecal BAs in 2 different groups, HC (n=35) and the patients with NAFLD-ELE (n=26). (C) The levels of BA synthesis, bile acid transport, and hepatic acid regulation related genes NCTP, Cyp7A1, SHP, and FXR in the mouse liver (n=5). (D) The levels of intestine barrier related genes occludin and Zo-1 in the mouse intestine (n=5). (E) Trans-epithelial electrical resistance assay using Caco2 cell. Caco-2 cells were co-incubated with 200 μl of OD600 0.3

bacterial suspension (7□107 CFU/ml) in MEM media for 8 hrs and the TEER was measured respectively, And the levels of endotoxin level in mouse serum (n=5) using LAL assay kit. (F) The levels of glucose, xylose, fructose, galactose and mannose in different diet groups (n=4-7).

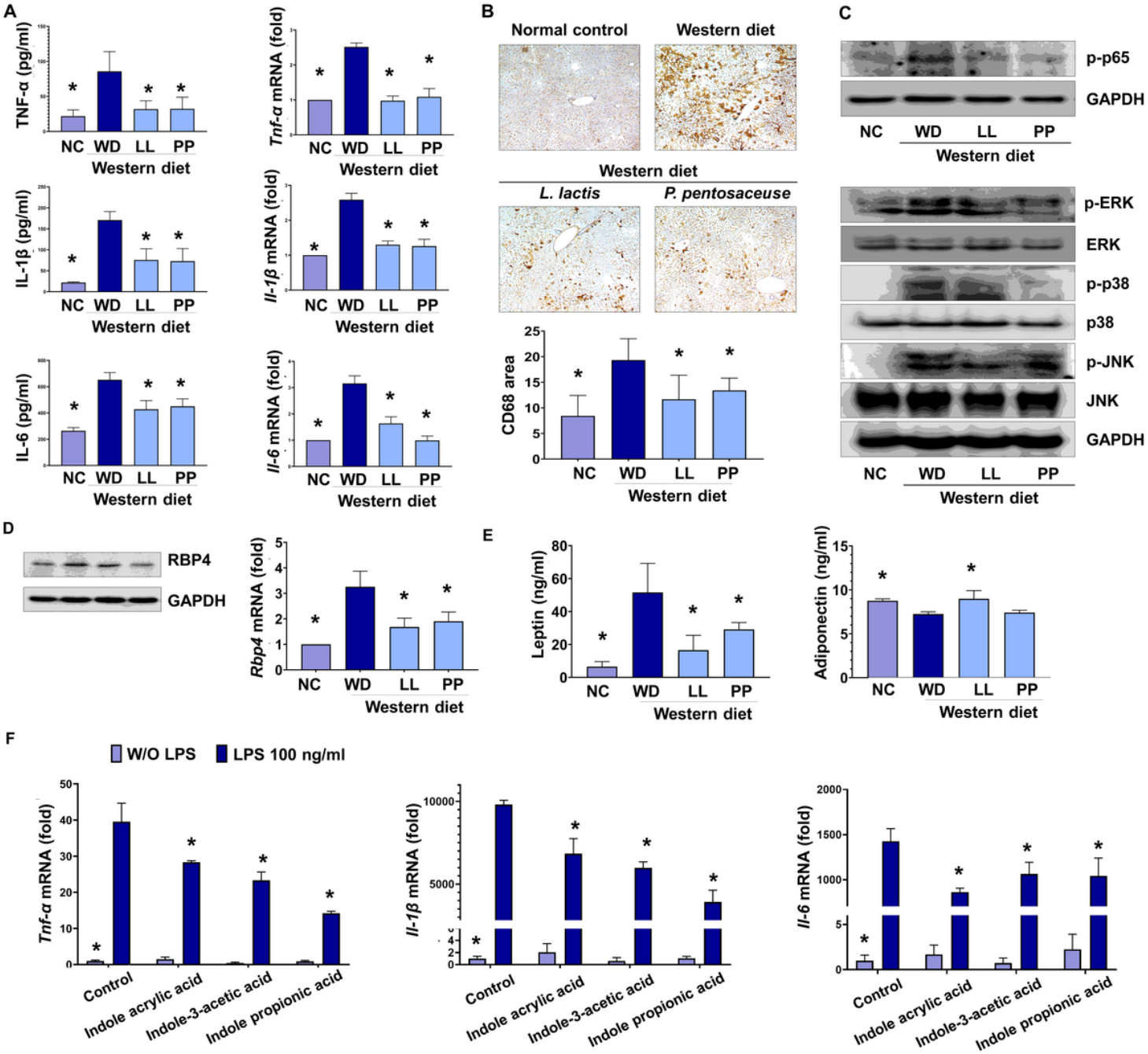

Figure 7

Effect of L. lactis and P. pentosaceus on the Western diet-induced inflammatory signaling pathways. (A) The levels of inflammatory cytokines TNF-α, IL-1β and IL-6 in the mouse liver (n=5). Inflammatory cytokine protein and mRNA analysis using ELISA and qRT-PCR. (B) Representative microphotographs and measured areas of CD68 immunohistochemistry. (C) Effect of probiotics on WD-induced activation of MAPKs and NF-kB in mouse liver. Mouse liver analyzed for the phosphorylated p65 and GAPDH,

phosphorylated and total forms of ERK, p38, and JNK MAPKs by Western blotting using specific antibodies. (D) The level of retinol binding protein 4 (RBP4) protein and mRNA analysis using Western blotting and qRT-PCR. Mouse liver analyzed for the RBP4 and GAPDH by Western blotting using specific antibodies. (E) The analysis of adipokines leptin and adiponectin in mouse liver (n=5) using ELISA kit. (F) Raw 264.7 cell was treated iondole acrylic acid (100 μM), Indole-3-acetic acid (500 μM), and Indole-propionic acid (100 μM) with LPS (100ng/ml). After 3 hours, inflammatory cytokine gene expression analysis using qRT-PCR. *p < 0.05 as compared with WD.

A

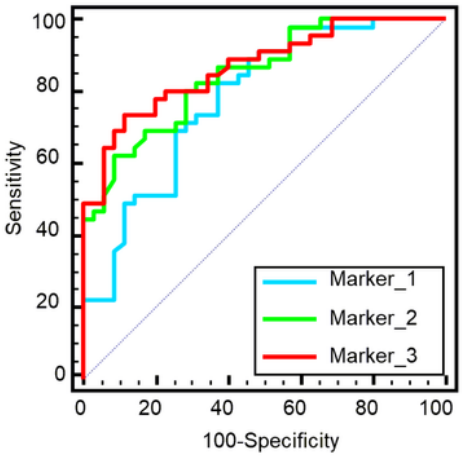

	Variable	AUC (95% CI)	Sensitivity	Specificity	SE
Marker_1	Indole-3-propionic acid	0.782 (0.676-0.867)	82.22	62.86	0.0523
Marker_2	Indole-3-propionic acid, Chenodeoxycholic acid, Butyrate	0.846 (0.748-0.917)	62.22	91.43	0.0417
Marker_3	Indole-3-propionic acid, Chenodeoxycholic acid, Butyrate, Indole-3-butyric acid, Taurocholic acid, Taurochenodeoxycholic acid	0.868 (0.773-0.933)	73.33	88.57	0.0387

B

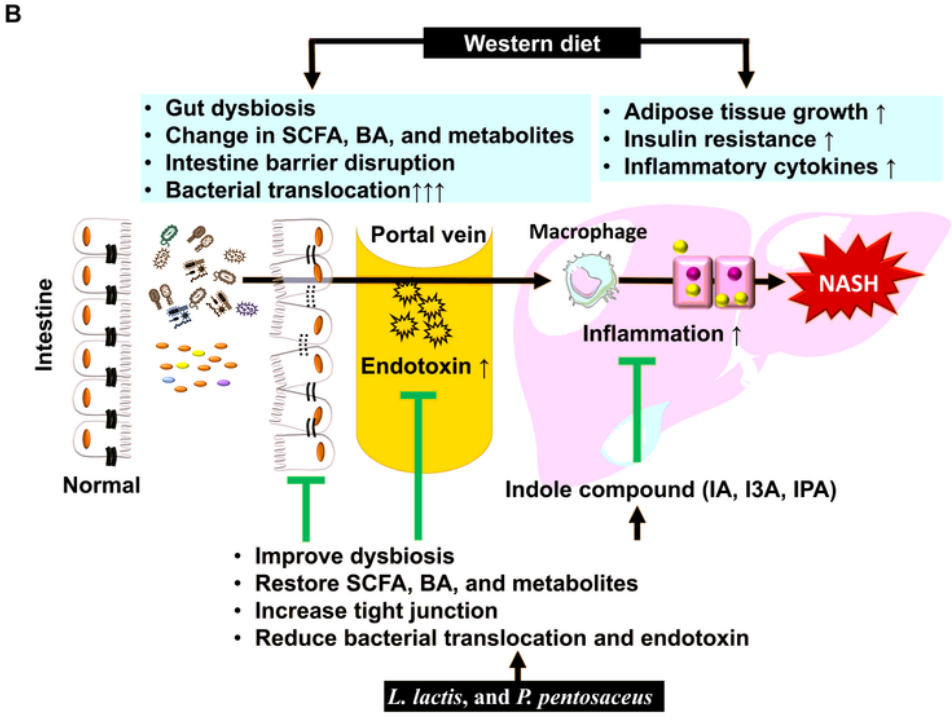

Figure 8

Performance of the metabolic biomarker panel for discriminating nonalcoholic steatohepatitis and summary. (A) ROC curve analysis of biomarker panel included by a single or multi fecal metabolites for discriminating the NCs (n=35) and NAFLD-ELE (n=45). Each biomarker cluster includes: Marker_1, Marker_2, and Marker_3. Optimal cutoff is determined using the closest to top-left corner and the 95% confidence interval is calculated using 1,000 bootstrappings. (B) Graphical summary.

Supplementary Files

This is a list of supplementary files associated with this preprint. Click to download.

- Supplementarydata.docx